400 mL of 100 mM potassium phosphate buffer (pH 7.3) until the dialysate contained no more radioactivity (about five changes). The sample was next microdialyzed against 6 M urea (9 mL, pH 7.0) for a period of 14 h. The dialysate was lyophilyzed, and the residue was taken up in water (4 mL). Enough solid trichloroacetic acid was added to give a 10% (w/v) solution. The sample was then analyzed as described in Figure 1.

Transamination of γ-Vinyl GABA by GABA Aminotransferase. Varying concentrations of GABA aminotransferase (0.07–0.13 units) were incubated with 15 mM γ-vinyl GABA in 50 mM potassium pyrophosphate buffer (pH 8.5) at 25 °C containing 2.6 mM [5-^{14}C]-α-ketoglutarate (Amersham; specific activity 0.803 mCi/mmol). A sample containing no enzyme and one containing no inactivator served as controls. After the enzyme in the samples containing inactivator had lost its activity as compared to the control without inactivator, all the samples were quenched with 20% (w/v) aqueous solution of trichloroacetic acid (30 μL each) and then applied to a column (0.6 cm × 5.5 cm) of Dowex 50W-X8 (H^+ form). The column was washed with 5 mL of water and 6 mL of 2 N aqueous ammonia. The last 5 mL of the ammonia eluate was found to contain all of the [^{14}C]glutamate. The glutamate containing eluate was measured for radioactivity content.

Equivalents of Nonamines Generated upon Inactivation of GABA Aminotransferase by [6-^{14}C]-γ-Vinyl GABA. Varying concentrations of GABA aminotransferase (0.2–0.46 units) were incubated with 1.05 mM [6-^{14}C]-γ-vinyl GABA, 3.97 mM α-ketoglutarate in 100 mM potassium phosphate buffer (pH 7.3) at 25 °C. A sample containing no enzyme and one containing no inactivator served as controls. After the enzyme in the samples containing inactivator had lost their activity as compared to the control without inactivator, solid trichloroacetic acid was added to one of the samples to make it a 10% (w/v) solution. After a period of 2 h, the samples and controls were applied separately to a column (0.6 cm × 5.5 cm) of Dowex 50W-X8 (H^+ form). The columns were washed with water and eight 5-mL fractions were collected and measured for radioactivity content.

Equivalents of 4-Oxohexanoic Acid (12a) and 4-Oxo-5-hexenoic Acid (6a) Generated during Inactivation of GABA Aminotransferase by [6-^{14}C]-γ-Vinyl GABA. GABA aminotransferase (1.28 units) was incubated with 1.04 mM [6-^{14}C]-γ-vinyl GABA, 2.7 mM α-ketoglutarate in 100 mM potassium phosphate buffer (pH 7.3) at 25 °C. A sample containing no enzyme and one containing no inactivator served as controls. After the enzyme in the samples containing inactivator had lost its activity as compared to the control without inactivator, **6a** and **12a** were added as standards, and the samples were injected separately onto a C18 reversed-phase analytical column (λ = 214 nm) using 100 mM sodium phosphate (pH 6) as eluant at a flow rate of 0.9 mL/min. Under these conditions the T_R of **12a** and **6a** were 14 and 11 min, respectively. Fractions were collected and analyzed for radioactivity content.

Acknowledgment. The authors are grateful to the Marion Merrell Dow Research Institute, Marion Merrell Dow, Inc. for a generous gift of γ-vinyl GABA and [6-^{14}C]-γ-vinyl GABA and to the National Institutes of Health (NS 15703) for financial support of this research.

Carbon Assignments and Heteronuclear Coupling Constants for an RNA Oligonucleotide from Natural Abundance ^{13}C–^{1}H Correlated Experiments[1]

Gabriele Varani and Ignacio Tinoco, Jr.*

Contribution from the Department of Chemistry and Laboratory of Chemical Biodynamics, University of California, Berkeley, California 94720. *Received April 8, 1991*

Abstract: Complete assignments of the proton-linked carbons for the oligoribonucleotide 5′(GGACUUCGGUCC) have been obtained from 2D ^{13}C–^{1}H correlated experiments at natural abundance. High-quality spectra have been collected at RNA concentrations commonly used in proton experiments (2 mM). Heteronuclear one-bond scalar couplings have been measured from high-resolution spectra. The results demonstrate the editing power of the ^{13}C–^{1}H correlation in the very crowded sugar region of the proton NMR spectrum of RNA. Thus, 2D ^{13}C–^{1}H correlated experiments can be one of the main tools used for RNA proton spectral assignments. Both the carbon chemical shifts and the ^{13}C–^{1}H couplings are shown to be sensitive to the conformation of the sugar and the phosphodiester backbone, previously characterized for this oligoribonucleotide using proton and phosphorus NMR data. The potential of ^{13}C NMR in the structural analysis of RNA is evident from the data reported here.

Structural studies of RNA oligonucleotides by NMR spectroscopy are severely limited by the spectral overlap of the crowded sugar proton region. Spectral assignments are difficult, and the crucial information on the phosphodiester backbone conformation contained in scalar couplings and NOEs involving sugar protons may be impossible to obtain.[2] Complete proton and phosphorus spectral assignments have been obtained for an RNA 12-mer (~4000 Da) from a combination of homo- and heteronuclear (^{31}P–^{1}H) correlated experiments and NOE spectroscopy.[3,4] At larger molecular weight, the overlap of the sugar protons makes it increasingly difficult to use correlated techniques for assignments and structural analysis. With the exception of the H1′, all other sugar protons resonate between 4 and 5 ppm; thus, assignments and the extraction of constraints for structural analysis are very difficult tasks. So far, one has had to rely mostly on NOESY-based information above 5000–6000 Da;[5] this information necessarily relies on conformational assumptions. Carbon NMR can help overcome these problems by editing the proton chemical shifts in 3D experiments on uniformly or selectively[6,7] labeled com-

(1) Abbreviations used: NMR, nuclear magnetic resonance spectroscopy; ppm, parts per million; 1D, 1-dimensional; 2D, two-dimensional; 3D, three-dimensional; NOE, nuclear Overhauser effect; NOESY, nuclear Overhauser effect spectroscopy; TPPI, time proportional phase incrementation; TSP, (trimethylsilyl)propionic acid; RNA, ribonucleic acid.

(2) (a) Altona, C. *Recl. Trav. Chim. Pays-Bas* **1982**, *101*, 413–433. (b) Wüthrich, K. *NMR of Proteins and Nucleic Acids*; Wiley: New York, 1986.

(3) Cheong, C.; Varani, G.; Tinoco, I., Jr. *Nature* **1990**, *346*, 680–682.

(4) Varani, G.; Cheong, C.; Tinoco, I., Jr. *Biochemistry* **1991**, *30*, 3280–3289.

(5) (a) Varani, G.; Wimberly, B.; Tinoco, I., Jr. *Biochemistry* **1989**, *28*, 7760–7772. (b) Puglisi, J. D.; Wyatt, J. R.; Tinoco, I., Jr. *Biochemistry* **1990**, *29*, 4215–4226. (c) Puglisi, J. D.; Wyatt, J. R.; Tinoco, I., Jr. *J. Mol. Biol.* **1990**, *214*, 437–453.

(6) (a) Kline, P. C.; Serianni, A. S. *J. Am. Chem. Soc.* **1990**, *112*, 7373–7381. Manoharan, M.; Gerlt, J. A.; Wilde, J. A.; Withka, J. M.; Bolton, P. H. *J. Am. Chem. Soc.* **1987**, *109*, 7217–7219.

(7) (a) Williamson, J. R.; Boxer, S. G. *Biochemistry* **1989**, *28*, 2819–2831. (b) *Ibid.* 2831–2836.

0002-7863/91/1513-9349$02.50/0

pounds, as demonstrated for proteins.[8] Until ^{13}C-labeled RNA oligonucleotides become available, ^{13}C–^{1}H experiments must be performed at natural abundance.

Natural abundance ^{13}C–^{1}H experiments on deoxyoligonucleotides[9] or very small model oligoribonucleotides[10] have been obtained in the past at relatively high nucleic acid concentrations, 10 mM or more. Conventional ^{1}H–^{1}H 2D high-field spectra are instead acquired at much lower RNA concentrations, 1–2 mM. The low efficiency of enzymatic[11] or organic RNA synthesis makes it difficult to obtain large amounts of oligoribonucleotides. Furthermore, limited solubility is often a problem, particularly for guanosine-rich sequences. Unusual and biologically important intramolecular structures can also be replaced by aggregates of intermolecular complexes at high RNA concentration. If high-quality 2D heteronuclear spectra could be obtained at the same RNA concentrations as homonuclear studies, ^{13}C–^{1}H experiments would become one of the main tools for spectral assignments in RNA oligonucleotides. Each sugar proton can be identified as an H2′, H3′, H4′, or H5′–H5″ from the favorable chemical shift dispersion in the carbon dimension,[10] overcoming one of the most difficult steps in spectral assignments.

We have investigated a 12-mer oligoribonucleotide 5′-(G_1GACUUCGGUCC$_{12}$) by natural abundance 2D ^{13}C–^{1}H correlation spectroscopy. Nearly complete assignments of the ^{13}C spectrum have been obtained from the available proton assignments. The relation between ^{13}C–^{1}H couplings, carbon chemical shifts,[10,12] and RNA conformation was investigated using the well-defined structure previously obtained by distance geometry from proton and phosphorus NMR data.[3,4] Following the studies on very small (2–3 nucleotides) model compounds,[10] this work presents the first example of the assignment of the ^{13}C spectrum for an RNA oligonucleotide. The use of ^{13}C NMR should prove indispensable in attempts to extend the structural investigation by NMR to oligoribonucleotides in the 5000–10000 molecular weight range.

Results

A 2D ^{13}C–^{1}H correlated spectrum for the RNA 12-mer acquired with carbon broad-band decoupling is shown in Figure 1. The doublets in the bottom left corner of the spectrum result from incomplete decoupling of purine C8–H8 cross-peaks. The very large coupling (~220 Hz) and the offset from the carrier (over 5000 Hz) cause the purine H8 resonances to be incompletely ^{13}C-decoupled by the GARP1 sequence. The most remarkable feature of the spectrum is the large dispersion of the cross-peaks in the carbon dimension when compared to the overlap in the proton dimension. The single adenine C2 is at the downfield edge of the spectrum, well separated from the pyrimidine C6 and purine C8 resonances that are approximately 15 ppm upfield. The pyrimidine C6 resonances are usually downfield from purine C8 resonances. Sugar H1′ and base H5 resonances superimpose in the proton spectrum between approximately 5 and 6 ppm, but the C5 carbons resonate downfield from the C1′ resonances. The spectrum of Figure 1 also reveals that cytosine and uracil C5's resonate in distinct spectral regions, approximately 5 ppm apart. These observations have important implications for the assignment of RNA proton spectra. In the past, deuteration at UH5, AH8 and, less frequently, AH2 positions was used to distinguish adenine

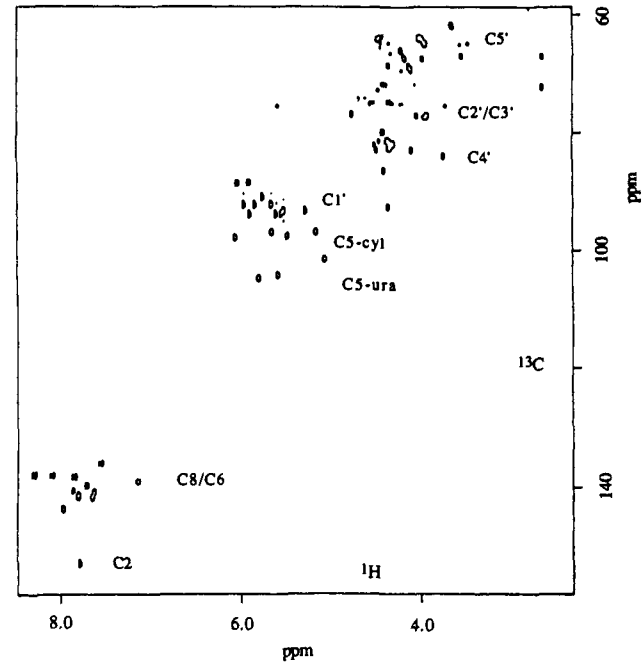

Figure 1. Carbon-decoupled ^{13}C–^{1}H COSY for the oligoribonucleotide 5′(G_1GACUUCGGUCC$_{12}$) in 2 mM sodium phosphate/0.01 mM EDTA at pH 6.7 and 25 °C; the RNA concentration is ~2 mM. The spectrum was acquired as described in the Experimental Section with a tuning delay of 2.5 ms to optimize the intensity of cross-peaks involving the base protons ($\tau = (2J)^{-1}$ for J = 200 Hz) and with the conventional phase cycling scheme.[16] Broad-band ^{13}C-decoupling during acquisition was performed with the GARP1 sequence.[18] Filtering was done with 3- and 5-Hz line-broadening in the ^{1}H and ^{13}C dimensions, respectively, after applying 30° shifted sine bells in both dimensions. 210 FIDs of 600 scans each were collected with a delay of 1.3 s between scans for a total acquisition time of 45 h.

H2 from other purine resonances[13] and to distinguish cytosine and uracil base protons.[5c] Work-intensive deuteration procedures can be replaced by 2D ^{13}C–^{1}H correlated experiments.

The editing power of the carbon is most evident for the sugar region of the spectrum. While sugar protons resonate in a narrow spectral region (approximately 3.9 to 4.6 ppm), the carbon resonances are spread over 20 ppm. Furthermore, different sugar carbon resonances are found in separate regions of the spectrum: the C4′ resonances are downfield, followed by the C2′ and C3′, with the C2′ generally, but not always, downfield, and the C5′ resonances at the upfield edge of the RNA carbon spectrum.

Sequence-specific carbon assignments for base and C1′ resonances were obtained from the spectrum shown in Figure 1 and its fully coupled version using the available proton assignments.[4] Assignment of the sugar carbons required spectra with higher resolution in both the carbon and proton dimensions to distinguish nearly overlapped cross-peaks. This was achieved by restricting the observation window to the sugar region, between approximately 6.5 and 3 ppm in the proton dimension and between 100 and 60 ppm in the carbon dimension (Figure 2). The aromatic resonances are far away from the sugar resonances, and their observation requires large spectral widths (~5000 Hz for ^{1}H and ~20000 Hz for ^{13}C at 600 MHz). By restricting the observation to the sugar region, the spectral widths could be reduced to 2000 Hz (^{1}H) and 6250 Hz (^{13}C), allowing a resolution of ~2 Hz/point in ω_2 and ~6 Hz/point in ω_1.

A subsection of the spectrum of Figure 2 containing the sugar H1′ and cytosine C5 resonances is shown in Figure 3a; cross sections at two representative carbon frequencies are shown in Figure 3b. Use of a $\tau = (2J)^{-1}$ delay to refocus the heteronuclear coupling before starting acquisition has some advantages, as is evident from Figure 3a,b. The refocusing delay is not strictly necessary in the absence of carbon decoupling, but its use prevents

(8) (a) Griesinger, C.; Sørensen, O. W.; Ernst, R. R. *J. Magn. Reson.* **1989**, *84*, 14–63. (b) Zuiderweg, E. R. P.; McIntosh, L. P.; Dahlquist, F. W.; Fesik, S. W. *J. Magn. Reson.* **1990**, *86*, 210–216. (c) Fesik, S. W.; Zuiderweg, E. R. P. *Quart. Rev. Biophys.* **1990**, *23*, 97–131.

(9) (a) Leupin, W.; Wagner, G.; Denny, W. A.; Wüthrich, K. *Nucleic Acids Res.* **1987**, *15*, 267–275. (b) Laplante, S. R.; Ashcroft, J.; Cowburn, D.; Levy, G. C.; Borer, P. N. *J. Biomol. Struct. Dyn.* **1988**, *5*, 1089–1099. (c) Ashcroft, J.; Live, D. H.; Patel, D. J.; Cowburn, D. *Biopolymers* **1991**, *31*, 45–55.

(10) (a) Lankhorst, P. P.; Erkelens, C.; Haasnoot, C. A. G.; Altona, C. *Nucleic Acids Res.* **1983**, *11*, 7215–7230. (b) Stone, M. P.; Winkle, S. A.; Borer, P. N. *J. Biomol. Struct. Dyn.* **1986**, *3*, 767–781.

(11) Milligan, J. F.; Groebe, D. R.; Witherell, G. W.; Uhlenbeck, O. C. *Nucleic Acids Res.* **1987**, *15*, 8783–8798.

(12) Santos, R. A.; Tang, P.; Harbison, G. S. *Biochemistry* **1989**, *28*, 9372–9378.

(13) Wimberly, B.; Chastain, M. Unpublished results.

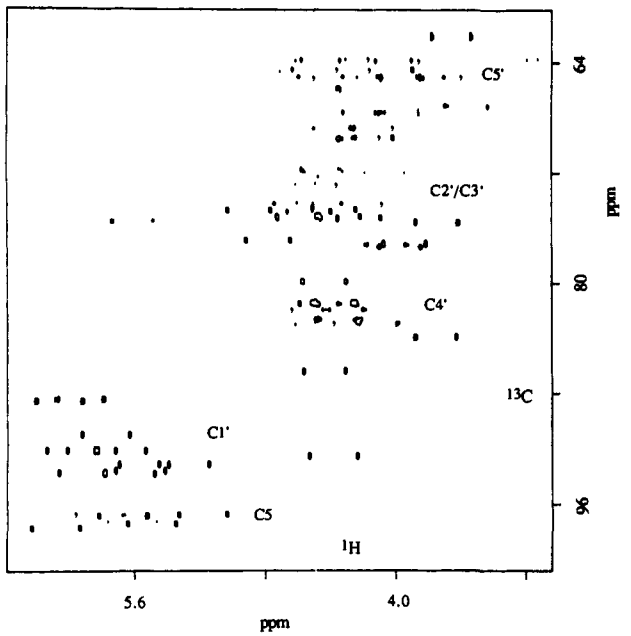

Figure 2. Coupled ^{13}C-^{1}H COSY spectrum acquired on the same sample as Figure 1. The observation window was restricted to the sugar region, resulting in greatly improved spectral resolution (2 Hz/point in the proton dimension, 6 Hz/point for carbon after zero-filling to 1K real points in the ω_1 dimension). Folded aromatic resonances were eliminated by audio filtering with a cutoff of 2500 Hz from the carrier; folded H5–C5 cross-peaks from two uracils are observed as weak out-of-phase cross-peaks close to the cytosine H5–C5 resonances. The tuning delay was 3 ms and filtering was done with 1- and 5-Hz line-broadening in the ^{1}H and ^{13}C dimensions, respectively, after applying 30° shifted sine bells in both dimensions. 160 FIDs of 288 scans each were collected with a delay of 2.5 s between scans for a total acquisition time of 33 h. A more recent phase cycling scheme considerably improved the suppression of artifacts at the lower edge of the spectrum.[17]

Table I. Carbon Chemical Shifts (Relative to TSP) for the Oligoribonucleotide 5′(G_1GACUUCGGUCC$_{12}$) (25 °C in 2 mM Sodium Phosphate/0.01 mM EDTA, pH 6.7)

	C8/6	C2/5	C1′	C2′	C3′	C4′	C5′
5′G_1	137.5	na	90.6	74.3	73.6	82.6	65.7
G_2	135.5	na	91.9	74.8	(*a*)	81.6	65.2
A_3	137.8	152.0	91.9	74.9	(*a*)	81.1	64.2
C_4	138.5	96.5	92.9	74.9	71.5	(*b*)	64.5
U_5	139.2	103.8	93.5	75.3	72.5	81.6	63.1
U_6	143.0	104.3	88.2	74.2	77.0	86.1	67.2
C_7	141.1	97.5	88.3	76.9	79.5	83.7	66.7
G_8	141.2	na	93.5	76.6	75.1	(*b*)	68.4
G_9	137.5	na	92.2	74.3	73.8	(*b*)	69.0
U_{10}	140.6	101.1	93.3	74.5	71.4	(*b*)	63.2
C_{11}	140.1	96.6	92.9	74.9	71.6	(*b*)	63.8
C_{12}	140.2	97.2	91.9	76.8	69.2	82.6	64.3

[a] One resonance at 72.0 ppm, the other at 72.4 ppm. [b] Two resonances at 82.5 ppm, three others at 81.1 ppm.

the cancellation of antiphase components from different cross-peak pairs accidentally superimposed.

All C2′ and C3′ carbons were assigned from the spectrum of Figure 2, with the exception of two H3′–C3′ cross-peaks, superimposed in the proton dimension and therefore indistinguishable. All but five C4′ carbons were also assigned, the missing resonances being superimposed in both the proton and carbon dimensions. All C5′ resonances were unambiguously identified in the upfield section of the spectrum. Assignment of the C5′ resonances lends conclusive support to the assignment of the H5′ and H5″ protons on the basis of proton and phosphorus data;[4] this has been rarely achieved in the past for either RNA or DNA oligonucleotides. The carbon assignments are reported in Table I.

One-bond ^{13}C-^{1}H scalar couplings were measured from fully coupled experiments and are reported in Table II. The accuracy

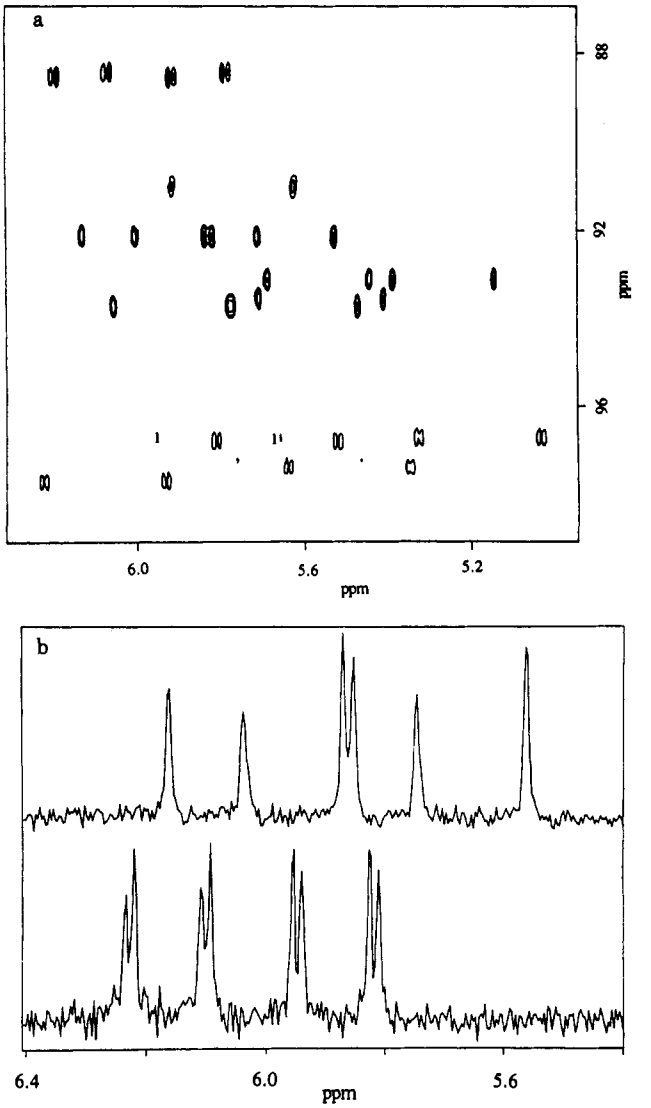

Figure 3. (a) Subsection of the same spectrum as Figure 2, containing cross-peaks between sugar H1′–C1′ and cytosine H5–C5 resonances. (b) One-dimensional proton slices at 88.2 (bottom) and 92.1 (top) ppm (^{13}C) illustrate the sensitivity obtainable at just a 2 mM oligoribonucleotide concentration.

Table II. One-Bond ^{13}C-^{1}H Scalar Couplings (Hz) for the Oligoribonucleotide 5′(G_1GACUUCGGUCC$_{12}$) (25 °C in 2 mM Sodium Phosphate/0.01 mM EDTA, pH 6.7)[a]

	8/6	2/5	1′	2′	3′	4′	5′/5″
5′G_1	221	na	174	157	149 ± 2	146	≈150/150
G_2	220	na	175	≈160		145	≈150/145
A_3	218	205	175	≈160		≈145	149/146
C_4	183	175	180	159	143		≈150/145
U_5	184	178	182 ± 2	155	≈145	147	≈145/145
U_6	186	178	170	147 ± 2	152	154	≈145/145
C_7	181	175	169	≈150	160	151	≈145/150
G_8	219	na	169 ± 2	162	149		≈145/145
G_9	222	na	174	158	147		≈145/145
U_{10}	182	177	179	161	≈145		≈150/145
C_{11}	180	174	179	159	≈140		≈150/145
C_{12}	185	174	175	156	144	≈145	≈150/145

[a] Uncertainties are ±2 Hz for the base protons and ±1 Hz for the sugar protons, unless otherwise indicated; the ≈ symbol refers to semiquantitative estimates of the coupling.

of the coupling constants was estimated by comparing splittings obtained from different 1D slices of the 2D spectrum, directly from the two-dimensional spectra, and by comparing the results of spectra with different resolution. Couplings could be measured very accurately from cross-peaks with simple multiplet structures (H1′–C1′, H2′–C2′, most H4′–C4′, H8/6–C8/6, H5–C5, H2–

C2). It was more difficult to obtain H4′–C4′ couplings for C_3-endo sugar conformers because of the loss in sensitivity induced by the passive H3′–H4′ couplings. The task was even more difficult for the H3′–C3′, H5′–C5′, and H5″–C5′ cross-peaks, and this is reflected in larger uncertainties in Table II. The sensitivity is limited for cross-peaks involving H3′, H5′, and H5″ protons by the passive ^1H–^1H and ^{31}P–^1H couplings. Triply tunable probes would help by allowing phosphorus decoupling during acquisition.[10a] This would partially collapse the H3′, H4′, H5′, and H5″ multiplets by removing the small heteronuclear couplings that increase the apparent line width of these resonances.

Discussion

The first and most difficult step in the spectral analysis of RNA oligonucleotides is to identify the sugar protons as H2′, H3′, H4′, H5′, or H5″. This is generally an easy task with deoxyoligonucleotides, because DNA sugar protons resonate in clearly separated regions of the spectrum, with the exception of H4′, H5′, and H5″. However, for RNA, all sugar protons resonate between 4 and 5 ppm. It is also important to distinguish adenine H2's from purine H8 resonances, particularly in single-stranded regions where the common double helix connectivities that are the standard basis for spectral assignments are absent. Finally, distinguishing cytosine from uracil base protons can considerably simplify the assignment process. Some of these tasks were accomplished in the past by time-consuming selective deuteration experiments.[5c] The data presented here demonstrate that 2D ^{13}C–^1H correlated spectra can overcome the need to prepare deuterated samples and provide information not obtainable from proton NMR alone. Very high-quality ^{13}C–^1H correlated spectra were obtained at ~2 mM RNA concentration (Figures 1 and 2). This concentration is comparable to those commonly used for 2D ^1H–^1H experiments, well below the concentrations of previous studies on deoxyoligonucleotides[9] and small-model oligoribonucleotides (≥ 10 mM).[10] The excitation sequence in the 2D experiment relies on the transfer of the proton magnetization to the carbons to improve sensitivity. The "tuning delay" in the excitation sequence ($\tau = (2J)^{-1} = 2.5$–3 ms) is very short because of the large ^{13}C–^1H couplings. Relaxation will not degrade the sensitivity even at fairly large molecular weights. High-quality ^{13}C–^1H spectra have been obtained in this laboratory with oligonucleotides containing 25 to 27 nucleotides, corresponding to approximately 8000 Da.[13] Natural abundance ^{13}C–^1H correlated experiments are clearly very helpful and should be used routinely as one of the main tools for spectral assignments of RNA oligonucleotides.

Besides clearly separating the sugar resonances, the ^{13}C–^1H correlation also provides a way of identifying unusually shifted or severly overlapped resonances. This is demonstrated by the two resonances at 5.61 ppm (an H3′–C3′ resonance) and 4.38 ppm (H1′–C1′) (Figure 2). Both protons are shifted over 1 ppm from their normal positions by the anomalous ring current generated by a guanine base in the unusual syn conformation around the glycosidic angle.[4] The H3′ proton at 5.61 ppm was assigned after some difficulty from the very distinct pattern of coupling constants observed in ^1H–^1H and ^{31}P–^1H correlated spectra;[3,4] its assignment would have been greatly simplified had ^{13}C–^1H spectra been available at the time. The H1′ proton at 4.38 ppm had not been assigned before because of the accidental superposition with the H2′ proton from the same sugar, also at 4.38 ppm. Its identification is straightforward in the ^{13}C–^1H correlated spectra of Figures 1 and 2.

Empirical correlations between the properties of sugar and base carbons and RNA conformation were proposed from the temperature dependence of carbon chemical shifts for di- and trinucleotides.[10] Changes in carbon chemical shifts at increasing temperature were attributed to an increase in the population of the DNA-type C_2-endo sugar conformer, and to the loss of base–base stacking. The solution structure of the oligonucleotide investigated here has been determined at very high resolution from proton and phosphorus NMR using distance geometry.[3,4] The conformation is very unusual: two nucleotides adopt the C_2-endo sugar conformation commonly found in deoxyoligonucleotides; one base is in the syn conformation around the glycosidic angle; and the extent of base stacking and hydrogen bonding is very different for the loop ($-U_5UCG_8-$) and stem ($_5$-G_1GAC_4- and $-G_9UCC_3$-) nucleotides. This variability provides structural contrast and, consequently, the opportunity to reexamine the correlations proposed from very small model compounds. Since many effects can contribute to carbon chemical shifts, only carbon resonances which are shifted at least 2–3 ppm from average will be considered, without any attempt to justify smaller variations.

The chemical shifts of the base carbons for two out of twelve nucleotides are unusual. The C8 carbon from G_8 resonates ~4 ppm downfield from other purine C8's. The G_8 base is the only nucleotide in the syn conformation about the glycosidic angle;[3,4] the downfield shift of the C8 carbon from the G_8 guanine can be attributed to the unusual relative position of the base and the sugar. The G_8 sugar carbon resonances, in particular C1′, do not appear to be significantly affected by the syn base. We do not know of any previous observation concerning the unusual shift of base carbons for nucleotides adopting the syn conformation. The C6 carbon from the unpaired nucleotide U_6 is 2–3 ppm downfield from other pyrimidine C6's; the U_6 uracil is the only base facing the solvent and lacking significant base–base stacking interactions.[3,4] The downfield shift of the C6 carbon could be attributed to poor base stacking. This interpretation is consistent with quantum mechanical calculations suggesting that the larger size of carbons makes them more sensitive than protons to the effect of stacking interactions.[14]

The C1′ resonances for the two unpaired nucleotides, U_6 and C_7, are ~5 ppm upfield from other pyrimidine C1′ resonances (Figure 3a). For these two nucleotides, the sugar is in the DNA-like C_2-endo pucker;[3,4] for the other nucleotides, the sugar conformation is close to the classical C_3-endo pucker normally found in RNA double helices.[2] Conformational equilibrium is present for the nucleotides at both ends of the molecule, and the sugar pucker is a mixture of N-type (close to C_3-endo) and S-type (C_2-endo) conformers in fast exchange. This produces intermediate values for the chemical shifts of the C1′ carbons of G_1 and C_{12} (Table I). A 2–3 ppm upfield shift was reported for the C1′ resonances of small oligoribonucleotides undergoing the C_3-endo to C_2-endo transition at increasing temperature.[10a] The present results fully support the correlation between C1′ chemical shifts and sugar conformation but do not agree with results from solid-state ^{13}C NMR on fibrous DNA.[12] The C1′ resonances from B-form DNA fibers (with C_2-endo sugar) were downfield from those of A-form DNA fibers with C_3-endo sugar pucker. This disagreement could be due to the different behavior of carbon C1′ resonances in ribose and deoxyribose sugars.

Three C2′ resonances, from C_7, G_8, and C_{12}, are significantly shifted downfield from all other C2′ carbons, resonating at approximately 77 ppm (Table I). C_{12} is the terminal nucleotide, and several effects could explain this anomaly. Since the U_6 C2′ chemical shift is similar to that of other pyrimidine C2′ carbons, it is unlikely that the sugar conformation contributes significantly to the C2′ shift; this was also observed in di- and trinucleotides.[10] It is tempting to speculate that hydrogen bonds involving the 2′-hydroxy groups of C_7 and G_8 as either donors or acceptors might be responsible for the downfield shift of the corresponding carbons. Interactions involving 2′-hydroxy groups from the four central nucleotides (U_5UCG_8) have been shown to thermodynamically stabilize the unusual structure of this molecule.[15]

The upfield shift of the C_{12} C3′, ~2 ppm, is likely due to the absence of the phosphate group at the 3′ end of the molecule; upfield shifts are consistently observed for the H2′, H3′, and H4′ protons from 3′-terminal sugars in oligoribonucleotides. The downfield shifts of U_6 and C_7 are at least partially attributable to the C_2-endo conformation of the sugar. The 5–6 ppm downfield shifts reported in Table I are comparable to those observed in both

(14) Giessner-Prettre, C.; Pullman, B. *Quart. Rev. Biophys.* **1987**, *20*, 113–172.
(15) Sakata, T.; Hiroaki, H.; Oda, Y.; Tanaka, T.; Ikehara, M.; Uesugi, S. *Nucleic Acids Res.* **1990**, *18*, 3831–3839.

the liquid[10a] and the solid state[12] for the C3′ carbons of nucleotides undergoing the C_3-endo to C_2-endo conversion. This effect was attributed to steric interactions between H3′ and O5′; repulsion of the σ-bonding electrons toward the carbon ("steric compression") increases the diamagnetic shielding.[12] However, other conformational effects should be considered, since quantum mechanical calculations have suggested that the C3′ resonances can also be affected by the conformation of the C3′–O3′ backbone torsion angle.[14] The results of Table I do not clarify the correlation between C3′ chemical shifts and sugar and backbone conformation, because U_6 and C_7 adopt C_2-endo pucker but also have the unusual gauche$^-$ conformation for the C3′–O3′ torsion angles.

The downfield shifts of the C4′ carbons at C_2-endo puckered nucleotides (U_6 and C_7; see Table I) are consistent with previous reports revealing an ~3 ppm downfield shift when the sugar conformation changes from C_3-endo to C_2-endo.[10] Other effects are likely to play a role, however, since the downfield shift of U_6 is much larger than that of C_7. The results also suggest a correlation between the C5′ chemical shifts and the backbone conformation. The C5′ resonances of G_8 and G_9 are downfield from all other C5′ carbons; the normal double helix backbone conformation is abandoned to accommodate the syn G_8 base. However, the observed downfield shifts (~5 ppm) are 1 order of magnitude larger than those predicted from quantum mechanical calculations investigating the effect of the backbone degrees of freedom on the C5′ shielding.[14] A smaller but significant downfield shift, close to the 2 ppm previously reported,[10] is correlated with the C_3-endo to C_2-endo conversion at U_6 and C_7.

The variations in the scalar coupling data for different nucleotides (Table II) suggest that one-bond ^{13}C–^{1}H couplings are also sensitive to the oligonucleotide conformation. This is not surprising since the scalar interaction is electron-mediated and changes in conformation can affect the properties of the bonding electrons. The magnitude of these effects is not large: deviations from average are <20 Hz, or 10% of the total interaction energy. We are not aware of any proposed correlation between one-bond ^{13}C–^{1}H scalar couplings and oligonucleotide conformation. Small decreases in several ^{13}C–^{1}H coupling constants have been reported when netropsin binds deoxyoligonucleotides,[9c] but no structural explanation was proposed.

Scalar couplings involving base carbons do not appear to vary significantly throughout the molecule, but the sugar ^{13}C–^{1}H couplings differ for different nucleotides. C1′–H1′ couplings decrease from ~180 to ~170 Hz for G_8 when the glycosidic angle is syn. The values of 175–180 Hz for the C1′–H1′ couplings reported in Table II for most nucleotides are larger than those previously reported for DNA oligonucleotides with C_2-endo sugar pucker.[9] However, values very close to those observed in deoxyoligonucleotides, ~170 Hz, were found for the two nucleotides adopting the C_2-endo sugar conformation, U_6 and C_7. Variations in scalar couplings are more significant for the C2′–H2′ interaction. The coupling changes from 160 Hz for C_3-endo conformers to 145–150 Hz when the pucker is C_2-endo. The C3′–H3′ couplings appear instead to be larger for the C_2-endo puckered nucleotides, U_6 and C_7, than for the other nucleotides (Table II). It is impossible, however, to attribute this change solely to the sugar conformation; other conformational degrees of freedom, in particular the C3′–O3′ torsion angle, could also contribute significantly. The C3′–H3′ coupling (160 Hz) observed for C_7 is very close to the values reported for DNA oligonucleotides.[9] The C4′–H4′ couplings increase slightly (~5 Hz) for both U_6 and C_7 (Table II), probably as a consequence of the C_2-endo sugar conformation; very similar values (150–155 Hz) have been reported for deoxyoligonucleotides.[9] The accuracy of C5′–H5′ and C5′–H5″ couplings is insufficient to establish any trend.

In summary, the results of Table I and II demonstrate the sensitivity of the ^{13}C NMR properties to the conformation of RNA molecules. In accordance with previous reports,[10] the C1′ and C3′ sugar resonances were found to be clearly affected by the ribose conformation. The data presented here reveal that the base carbon shifts are sensitive to base stacking and to the relative position of the sugar and the base (the glycosidic angle). For the C2′, C4′, and C5′ carbons, several structural features appear to determine the carbon shifts and splittings, including the sugar and phosphodiester backbone conformation. More studies on well-characterized RNA structures are necessary in order to clarify the structural origin of the unusual shifts observed for some sugar carbons in this oligonucleotide. The data of Table II show that one-bond heteronuclear ^{13}C–^{1}H scalar couplings are also sensitive to conformation. These results should motivate further experimental investigations on oligonucleotides with well-defined conformations, as well as the theoretical analysis needed to understand the empirical correlations. The conformational effects on carbon chemical shifts and scalar couplings reported here are large and can be measured precisely at high molecular weight. This information has the potential to be of considerable help in structural studies of RNA molecules in the 10000–15000 Da range.

Experimental Section

The RNA oligonucleotide 5′pppG$_1$GAC(UUCG)GUCC$_{12}$ was synthesized enzymatically using T7 RNA polymerase and synthetic DNA templates,[11] and purified according to previously described procedures.[3-5] Approximately 8 mg of RNA was dialyzed against 2 mM sodium phosphate/0.01 mM EDTA (pH 6.7). The purified RNA was lyophilized several times in 99.8% D_2O and dissolved in 1 mL of 99.96% D_2O (Aldrich) to a final concentration of ~2 mM. Limited solubility prevented higher RNA concentrations; a visible precipitate formed when the sample was dissolved in the usual 0.4-mL sample volume. All NMR experiments were done on a Bruker AMX-600 spectrometer operating at 600 MHz for proton and 150.9 MHz for carbon, using a "reverse" probe. Data were transferred to a μVAX and processed using the program FTNMR (Hare Research, Inc).

Heteronuclear correlated spectra were acquired with or without carbon broad-band decoupling (cpd) using the pulse sequence:[16]

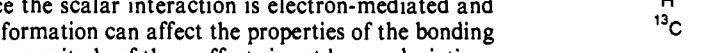

The delay τ was tuned to 2.5 ms for optimal excitation of aromatic resonances or 3 ms for enhancing the sugar resonances. The phases were cycled according to the standard phase cycle[16] or to a recently proposed scheme;[17] this second scheme considerably improved the suppression of artifacts at the lower edge of the spectrum. The carbon $\pi/2$ degree pulse lengths (17 μs for the high power pulse) were optimized using an aqueous ^{13}C-labeled glucose sample. Broad-band decoupling during acquisition was accomplished through the GARP1 sequence.[18]

2D NMR spectra were recorded in the phase-sensitive mode using the TPPI method to obtain pure absorption spectra[19] and preirradiation at low decoupler power of the residual HDO peak. All spectra were referenced using an internal TSP standard from the cross-peak at 0 ppm in both proton and carbon dimensions in the 2D spectra. 160–210 FIDs of 2K complex data points were collected. Repetition delays were 1.3–2.5 s, and 288–600 scans were averaged for each FID; longer repetition delays worked best. Acquisition times were 33–45 h. Data were zero-filled to 1K real points in t_1 and apodized using 30° phase-shifted sine bells in both dimensions; line-broadening contributions of 1–2 Hz (t_2) and 3–5 Hz (t_1) were also applied. The sweep widths were 5000 (^{1}H) and 20000 Hz (^{13}C) or 2000 Hz (^{1}H) and 6250 Hz (^{13}C). Acquisition times were t_1^{max} = 2.6 ms and t_2^{max} = 102.4 ms when acquiring full spectra, or t_1^{max} = 6.4 ms and t_2^{max} = 256 ms when only the sugar region was observed. When the observation was restricted to the sugar region (6.5–3.5 ppm for proton, 100–60 ppm for carbon), folded aromatic resonances were removed by audio filtering with a cutoff of 2500 Hz, just larger than the "optimal" Nyquist frequency (2000 Hz).[20] The figure captions give details about each individual experiment.

Spectra acquired with a reduced observation window obviously have higher resolution if the FID is sampled with the same number of points, but also have better sensitivity. The relative signal/noise ratio of two spectra acquired with the same total number of sample points and re-

(16) (a) Bax, A.; Griffey, R. H.; Hawkins, B. L. *J. Magn. Reson.* **1983**, *55*, 301–315. (b) Wagner, G. *Meth. Enzym.* **1989**, *76*, 93–113.
(17) Cavanagh, J.; Keeler, J. *J. Magn. Reson.* **1988**, *77*, 356–362.
(18) Shaka, A. J.; Barker, P. B.; Freeman, R. *J. Magn. Reson.* **1985**, *64*, 547–552.
(19) Marion, D.; Wüthrich, K. *Biochem. Biophys. Res. Commun.* **1983**, *113*, 967–974.
(20) Ernst, R. R.; Bodenhausen, G.; Wokaun, A. *Principles of Nuclear Magnetic Resonance in One and Two Dimensions*; Clarendon Press: Oxford, 1987; p 351–353.

laxation delays, and filtered identically, depends on the ratio of the two bandwidths.[20] If the audio filter cutoffs are set at the Nyquist frequency, that ratio becomes the ratio of the acquisition times (t_2^{max}). The relative sensitivity is approximately proportional to the ratio of the acquisition times divided by the ratio of the delays between pulses.[20] When the sweep width is reduced while acquiring the same number of sample points, the acquisition time increases from 102.4 to 256 ms; however, the delay between pulses, ~2.5 s, does not change significantly. Consequently, the sensitivity is improved by the square root of the ratio of acquisition times, $(256/102.4)^{1/2} \sim 60\%$. Intuitively, the signal/noise ratio improves because the noise bandwidth is reduced; the sensitivity increases because a larger portion of the spectrometer time is spent acquiring data rather than waiting for the spins to relax.

Acknowledgment. It is a pleasure to thank Mr. David Koh for synthesizing DNA templates and Ms. Barbara Dengler for managing the laboratory. This research was supported in part by the National Institutes of Health Grant GM 10840, the Department of Energy, Office of Energy Research, Office of Health and Environmental Research Grant DE-FG03-86ER60406, and through instrumentation grants from the U. S. Department of Energy, DE-FG05-86ER75281, and the National Science Foundation, DMB 86-09305 and BBS 86-20134.

Establishment of the Metal-to-Cysteine Connectivities in Silver-Substituted Yeast Metallothionein

Surinder S. Narula,[†] Rajesh K. Mehra,[§] Dennis R. Winge,[§] and Ian M. Armitage*[,†,∥]

Contribution from the Department of Molecular Biophysics and Biochemistry and Department of Diagnostic Radiology, Yale University School of Medicine, 333 Cedar Street, New Haven, Connecticut 06510, and Department of Biochemistry and Medicine, University of Utah Medical Center, Salt Lake City, Utah 84132. *Received April 26, 1991*

Abstract: To elucidate the three-dimensional solution structure of yeast copper-metallothionein (MT) from *Saccharomyces cerevisiae*, silver-substituted yeast metallothionein has been prepared as an isomorphic, NMR active, metal ion derivative. Using Ag-MT, ^1H-^{109}Ag heteronuclear multiple quantum coherence transfer (HMQC) experiments have been performed to identify the individual ^{109}Ag resonances and their associated cysteine ligands, respectively. Specific factors associated with the optimized execution of the ^1H-^{109}Ag HMQC experiments are identified and discussed. Analysis of the HMQC data has established the specific connectivities between 10 of the 12 cysteine residues and seven bound $^{109}Ag(I)$ metal ions. The data confirm the exclusive involvement of cysteine thiolates in metal coordination and indicate that a minimum of eight cysteines are involved as bridging, shared ligands. Additionally, the present data suggest the existence of a mixed coordination number (2 and 3) for the seven bound Ag(I) ions.

Introduction

The metallothioneins (MTs) are small, cysteine-rich polypeptides that bind both essential heavy metals (e.g., Cu and Zn), and nonessential metals (e.g., Cd and Hg). MT gene transcription is inducible by the same heavy metals that are subsequently found bound to the MT protein, thereby providing a mechanism for cells to protect themselves against metal stress/overload. This metal response occurs in all eukaryotic organisms and tissues that synthesize MT and is operative for the several different isoform genes that are frequently present in a single organism.

The yeast *Saccharomyces cerevisiae* contains a metallothionein encoded by the *CUP1* locus.[1-3] In most strains of this yeast, the *CUP1* gene is transcriptionally regulated by only Cu(I) and Ag(I) ions.[4] One strain of *S. cerevisiae* has been shown to regulate the *CUP1* gene expression by Cd(II) as well as Cu(I).[5] The *CUP1* locus functions in copper detoxification by regulating the free Cu(I) ion concentration within the cells. Disruption of the *CUP1* MT gene results in hypersensitivity to copper-mediated cytotoxicity.[6] Detoxification is achieved by sequestration of copper ions in a stable complex with MT.

The 12 cysteine residues in yeast MT are all believed to serve as ligands for the eight bound copper ions.[7,8] Luminescence studies revealed that the copper ions are in the Cu(I) valence state and are bound in a solvent-inaccessible environment.[8] The Cu(I) state was confirmed by X-ray absorption edge spectroscopy (EXAFS).[9] The X-ray absorption edge features were similar to those observed for three coordinate Cu(I) model complexes.[9,10] These observations led to a proposed structure of a distorted cubic Cu_8S_{12} polynuclear cluster in which each Cu(I) ion is trigonally coordinated and each cysteinyl thiolate bridges two Cu(I) ions.[9] No folding intermediates were observed in the Cu(I) reconstitution studies analogous to the domains of mammalian MT. Reconstitution studies confirmed that Cu(I) ions bind to MT in a cooperative, all-or-none manner but were not able to confirm the existence of a single polynuclear cluster.[8]

Although the primary sequence of yeast MT is only distantly related to mammalian MTs, its metal coordination properties are similar. Both classes of MTs bind copper as Cu(I) in clusters with

* Address correspondence to this author at the Department of Molecular Biophysics and Biochemistry, Yale University School of Medicine, 333 Cedar Street, P.O. Box 3333, New Haven, CT 06510-8024.
[†] Department of Molecular Biophysics and Biochemistry, Yale University.
[§] Department of Biochemistry and Medicine, University of Utah.
[∥] Department of Diagnostic Radiology, Yale University.

(1) Fogel, S.; Welch, J. W. *Proc. Natl. Acad. Sci. U.S.A.* **1982**, *79*, 5342-5346.
(2) Karin, M.; Najarian, R.; Haslinger, A.; Valenzuela, P.; Welch, J.; Fogel, S. *Proc. Natl. Acad. Sci. U.S.A.* **1984**, *81*, 337-341.
(3) Butt, T. R.; Sternberg, E. J.; Gorman, J. A.; Clark, P.; Hamer, D.; Rosenberg, M.; Crooke, S. T. *Proc. Natl. Acad. Sci. U.S.A.* **1984**, *81*, 3332-3336.
(4) Wright, C. F.; Hamer, D. H.; McKenney, K. *J. Biol. Chem.* **1988**, *263*, 1570-1574.
(5) Inouhe, M.; Hiyama, M.; Tohoyama, H.; Joho, M.; Murayama, T. *Biochem. Biophys. Acta* **1989**, *993*, 51-55.
(6) Hamer, D. H.; Thiele, D. J.; Lemontt, J. E. *Science* **1985**, *228*, 685-690.
(7) Winge, D. R.; Nielsen, K. B.; Gray, W. R.; Hamer, D. H. *J. Biol. Chem.* **1985**, *260*, 14464-14470.
(8) Byrd, J.; Berger, R. M.; McMillin, D. R.; Wright, C. F.; Hamer, D. H.; Winge, D. R. *J. Biol. Chem.* **1988**, *263*, 6688-6694.
(9) George, G. N.; Byrd, J.; Winge, D. R. *J. Biol. Chem.* **1988**, *263*, 8199-8203.
(10) Kau, L-S.; Spira-Solomon, D. J.; Penner-Hahn, J. E.; Hodgson, K. O.; Solomon, E. I. *J. Am. Chem. Soc.* **1987**, *109*, 6433-6442.

0002-7863/91/1513-9354$02.50/0